arXiv:nucl-ex/0606020v1 14 Jun 2006

Strange Particle Production and Elliptic Flow from CERES

J Milošević (for the CERES Collaboration)

Physikalisches Institut der Universität Heidelberg, D 69120, Heidelberg, Germany

E-mail: `jmilos@physi.uni-heidelberg.de`

Abstract. Elliptic flow measurements as a function of p_T of charged ($\pi^{\pm}$ and low-p_T protons) and strange (Λ and K^0_S) particles from Pb+Au collisions at 158 AGeV/c are presented, together with measurements of ϕ and K^0_S meson production. A mass ordering effect was observed. Scaling to the number of constituent quarks and transverse rapidity y_T^{fs} scaling are presented. The results are compared with results from the NA49 and STAR experiments and with hydrodynamical calculations. For the first time in heavy-ion collisions, ϕ mesons were reconstructed in the same experiment both in the K^+K^- and in the e^+e^- decay channels. The obtained transverse mass distributions of ϕ mesons are compared with results from the NA49 and NA50 experiments. The yield and the inverse slope parameter of the K^0_S mesons were reconstructed from two independent analyses. Our results are compared with those from the NA49 and NA57 experiments.

PACS numbers: 25.75.Ld, 25.75.Dw

Submitted to: *J. Phys. G: Nucl. Phys.*

1. Introduction

Elliptic flow is described by the differential second Fourier coefficient of the azimuthal momentum distribution $v_2(\mathcal{D}) = \langle\cos(2\phi)\rangle_{\mathcal{D}}$ [1, 2, 3]. The brackets denote averaging over many particles and events, and $\mathcal{D}$ represents a phase-space window in the (p_T, y) plane in which v_2 is calculated. The azimuthal angle ϕ is measured with respect to the reaction plane defined by the impact parameter vector $\vec{b}$ and the beam direction. For non-central collisions ($b \neq 0$), v_2 is an important observable due to its sensitivity to the EoS, and through it to a possible phase transition to the QGP. Since we could identify protons via dE/dx only at low p_T, the v_2 of the Λ is important because this is a baryon as well. In comparison to the elliptic flow of pions and K^0_S mesons the Λ flow can be used to check the mass ordering effect and for comparison to hydrodynamical predictions. Testing the differential flow measurements of different particle species against different scaling scenarios may yield additional information about the origin of flow.

As strangeness enhancement has been suggested as a signature of the deconfined stage [4], understanding of the ϕ and K^0_S meson production is important as here hidden and open strangeness are involved. The study of ϕ yields in different decay channels is important in light of a possible modification of the ϕ mass, width and the branching ratios near the phase boundary.

2. Experiment

The CERES experiment consists of two radial Silicon Drift Detectors (SDD), two Ring Imaging CHerenkov (RICH) detectors and a radial drift Time Projection Chamber (TPC). The CERES spectrometer covers $\eta = 2.05 - 2.70$ with full azimuthal acceptance. The two SDDs are located at 10 and 13 cm downstream of a segmented Au target. They were used for the tracking and vertex reconstruction. The purpose of the RICH detectors is electron identification. The new radial-drift TPC operated inside a magnetic field with a maximal radial component of 0.5 T providing a precise determination of the momentum. Charged particles emitted from the target are reconstructed by matching track segments in the SDD and in the TPC using a momentum-dependent matching window. A more detailed description of the CERES experiment can be found in [5]. For the flow analysis, we used $30{\cdot}10^6$ Pb+Au events at 158 AGeV/c collected in the year of 2000 data taking period. Of these, 91.2% were triggered on $\sigma/\sigma_{geo} \leq 7\%$, and 8.3% events with $\sigma/\sigma_{geo} \leq 20\%$. The ϕ meson analysis in the kaon (dilepton) channel used $24{\cdot}10^6$ ($18{\cdot}10^6$) events taken with the most central trigger.

3. Methods of strange particle reconstruction

The Λ particles were reconstructed via the decay channel $\Lambda \rightarrow p{+}\pi^-$ with a $BR = 63.9\%$ and $c\tau = 7.89$ cm [6]. Due to the late decay of the Λ particle, as candidates for Λ daughters, only those TPC tracks which have no match to a SDD track were chosen.

Partial particle identification (PID) was performed using dE/dx information from the TPC by applying a $\pm 1.5\sigma$ ($+1\sigma$) window around the momentum dependent Bethe-Bloch value for pions (protons). On the pair level, a p_T dependent opening angle cut is applied, in addition to a cut in the Armenteros-Podalanski variables ($q_T \leq 0.125$ GeV/c and $0 \leq \alpha \leq 0.65$) to suppress K^0_S. With these cuts values for $S/B \approx 0.04$ and $S/\sqrt{B} \approx 500$ were obtained [7].

The K^0_S particles were reconstructed via the decay channel $K^0_S \rightarrow \pi^+ + \pi^-$ with a $BR = 68.95\%$ and $c\tau = 2.68$ cm [6]. Partial PID for π^+ and π^- was performed by applying a $\pm 1.5\sigma$ window around the momentum dependent Bethe-Bloch energy loss value for pions. As the K^0_S particle comes from a primary vertex, a possibility to suppress fake track combinations is given by a cut (0.02 cm) on the radial distance between the point where the back extrapolated momentum vector of the K^0_S candidate intersects the $x - y$ plane and the primary vertex. In addition, a cut of 1 cm on the z-position of the secondary vertex was applied. In this approach, the values of $S/B \approx 0.92$ and $S/\sqrt{B} \approx 500$ were obtained [8, 7].

In order to remove the effect of autocorrelations, tracks which were chosen as candidates for daughter particles were not used for the determination of the reaction plane orientation. In the case of Λ particle reconstruction, the combinatorial background was determined by ten random rotations of positive daughter tracks around the beam axis and constructing the invariant mass distribution, while in the case of K^0_S particle reconstruction, the mixed event technique was used.

Λ (K^0_S) particles were reconstructed in y-p_T-ϕ bins. We used the area under the peak, obtained by fitting the invariant mass distribution with a Gaussian, to measure the yield of Λ (K^0_S) in a given bin. Plotting the yield versus ϕ for different p_T and y values one can construct the $dN_{\Lambda(K^0_S)}/d\phi$ distribution. Fitting these distributions with a function $c[1 + 2v'_2 \cos(2\phi)]$, it is possible to extract the observed differential v'_2 values. The obtained v'_2 coefficients were corrected for the reaction plane resolution via $v_2 = v'_2/\sqrt{2\langle\cos[2(\Phi_a - \Phi_b)]\rangle}$ [3]. Here, Φ_a and Φ_b denote the azimuthal orientations of reaction planes reconstructed from two random subevents. In the case of the $\pi^\pm$ elliptic flow analysis, subevents are formed from positive and negative pions separately. Using the method of subevents, correction factors were calculated for different centrality bins. In all 3 analyses (Λ, K^0_S and $\pi^\pm$) similar values were obtained. The corresponding resolution ranges from about 0.16 to 0.31, depending on the centrality.

Due to the small statistics of strange particles, the differential elliptic flow analysis was performed for only two centrality classes. The huge statistics of $\pi^\pm$ allowed to perform the differential elliptic flow analysis in six centrality bins. As we used the combination of data taken with different triggers, the centrality is characterized by a weighted mean centrality $\langle\frac{\sigma}{\sigma_{geo}}\rangle$ calculated using the numbers of TPC tracks as statistical weights [7].

4. Results

In Fig. 1 are shown the resulting p_T dependences of v_2 for three particle species. An increase of the elliptic flow magnitude *vs* p_T for all three particle species is visible. In the case of Λ elliptic flow, the absolute systematic error Δv_2, estimated from two different ways of Λ reconstruction, is $^{+0.001}_{-0.007}$ for $p_T < 1.6$ GeV/c and $^{+0.00}_{-0.02}$ for $p_T > 1.6$ GeV/c which is small compared to the statistical errors. Particles are accepted as $\pi^{\pm}$ if their TPC dE/dx is within a $\pm 1.5\sigma$ window around the nominal Bethe-Bloch value for pions. The HBT contribution to the $\pi^{\pm}$ elliptic flow is subtracted using the procedure described in [9]. Separately calculated elliptic flow of π^+ and π^- shows that the averaged difference between them is ≈ 0.003 in both η and y, which can be attributed to the contamination of protons in π^+ sample. Comparing results obtained from two independent analysis methods we concluded that the overall absolute systematic error in $\pi^{\pm}$ elliptic flow measurements is not bigger than 0.0036.

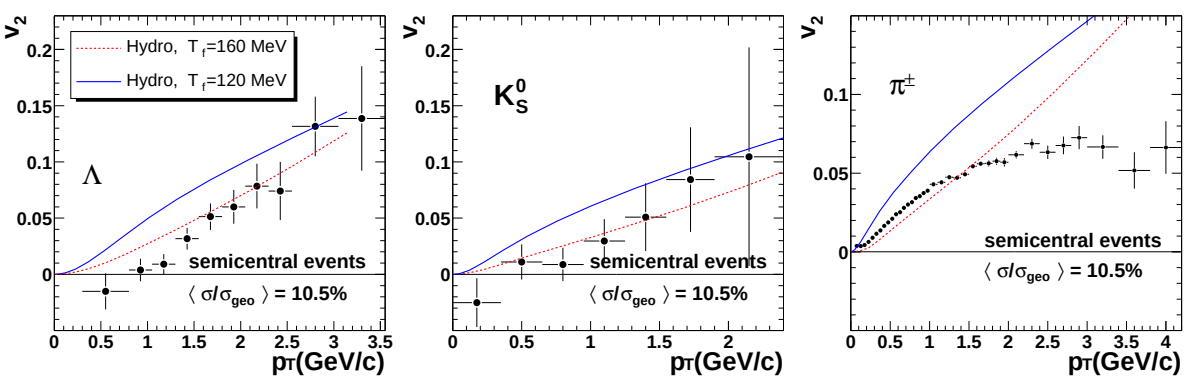

Figure 1. The Λ (left), K^0_S (middle) and $\pi^{\pm}$ (right) elliptic flow *vs* transverse momentum in semicentral events. Hydrodynamical predictions are presented for two freeze-out temperatures: $T_f = 120$ MeV (solid) and $T_f = 160$ MeV (dotted).

The elliptic flow results are compared with the hydrodynamical calculations done by P. Huovinen based on [10, 11]. The calculation was done in 2+1 dimensions with initial conditions fixed via a fit to the p_T spectra of negatively charged particles and protons in Pb+Pb collisions at 158 A GeV/c [12]. The underlying EoS assumes a first order phase transition to a QGP at a critical temperature of $T_c = 165$ MeV. The hydrodynamical predictions were calculated with 2 freeze-out temperatures, $T_f = 120$ MeV and $T_f = 160$ MeV. The model prediction with the lower freeze-out temperature of $T_f = 120$ MeV overpredicts the data, while rather good agreement can be achieved with a higher freeze-out temperature of $T_f = 160$ MeV (this is however not the preferred value considering the proton p_T spectra).

A comparison of the CERES data to results from NA49 [13] at the same energy ($\sqrt{s_{NN}} = 17$ GeV) and to STAR results [14] at $\sqrt{s_{NN}} = 200$ GeV is shown in Fig. 2. The NA49 and CERES data are in very good agreement. After rescaling the STAR results to the centrality used in the CERES experiment, the v_2 values measured at

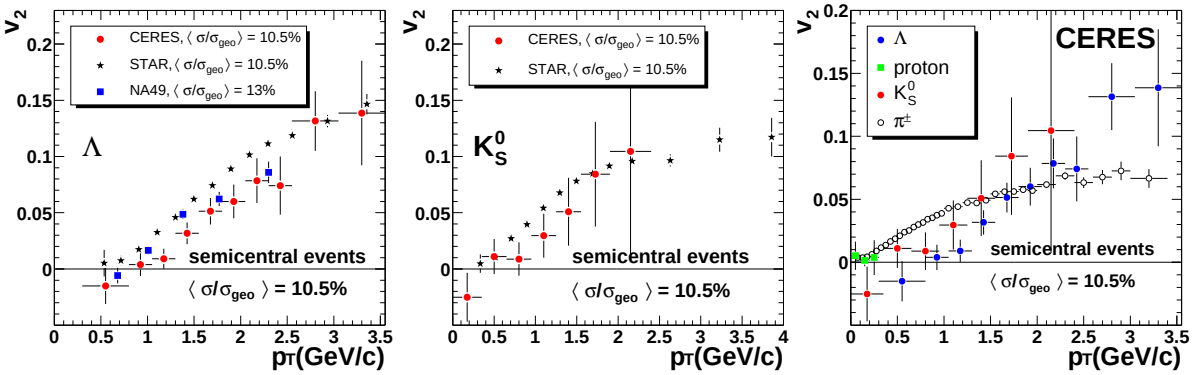

Figure 2. Comparison of Λ (left) and K^0_S (middle) elliptic flow measured by CERES, STAR and NA49. Comparison between the elliptic flow magnitude of the $\pi^{\pm}$, low-p_T protons, Λ, and K^0_S in semicentral events (right).

RHIC are $15-20\%$ higher due to the higher beam energy. In Fig. 2 (right), the elliptic flow magnitude of the $\pi^{\pm}$, K^0_S, low momentum protons, and Λ measured by CERES are compared. A mass ordering effect is observed. At small p_T, up to ≈ 1.5 GeV/c, $v_2(\Lambda) < v_2(K^0_S) < v_2(\pi^{\pm})$. In the region of high p_T, above ≈ 2 GeV/c, the tendency is the opposite. As proton and Λ hyperon have similar masses and 3 valence quarks each, the v_2 of low momentum identified protons is considered as a natural continuation of Λ $v_2(p_T)$ dependence in the region of small p_T. The indication of a possible undershoot to negative values is tantalizing but not significant in view of the statistical errors.

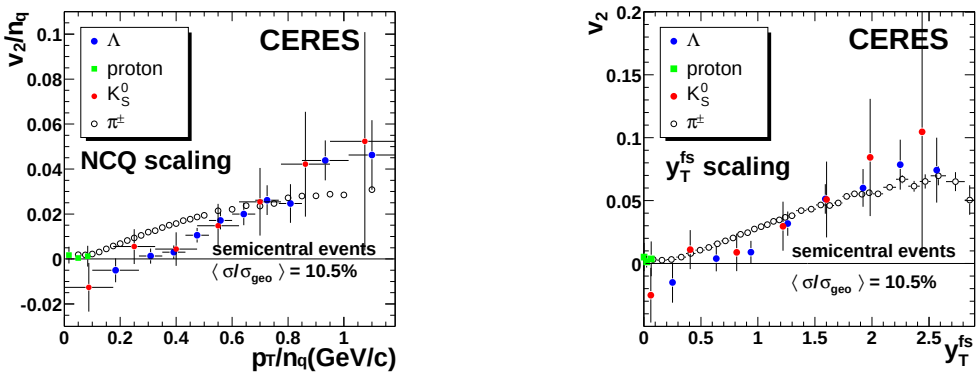

Figure 3. Comparison between the elliptic flow magnitude of $\pi^{\pm}$, low-p_T protons, Λ, and K^0_S scaled to the number of the constituent quarks (left) and to the y_T^{fs} variable (right).

Fig. 3 (left) shows the scaled elliptic flow magnitude v_2/n_q for $\pi^{\pm}$, K^0_S, low-p_T protons and Λ plotted against p_T/n_q in semicentral events. Here, n_q denotes the number of the constituent quarks. There is an indication that high p_T particles ($p_T > 1.5$ GeV/c) show scaling behavior. A similar behavior is observed by the STAR experiment at RHIC [14]. This is consistent with the coalescence mechanism where co-moving quarks with high p_T form hadrons. In this case scaling to the number of the constituent quarks

shows the original momentum space azimuthal anisotropy formed at the early stage of the collision.

Within the Buda-Lund model of hydrodynamics [15], a scaling of elliptic flow of different particle species has been suggested [17, 16] when instead transverse momentum the transverse rapidity is used. We use their scaling variable y_T^{fs} [18] and show, in Fig. 3 (right), the results for $\pi^{\pm}$, K_S^0, low-p_T protons and Λ in semicentral events. Within statistical errors a reasonable scaling is observed for all particles. This may indicate a hydrodynamic behavior of matter created in central heavy-ion collisions at the highest SPS energy.

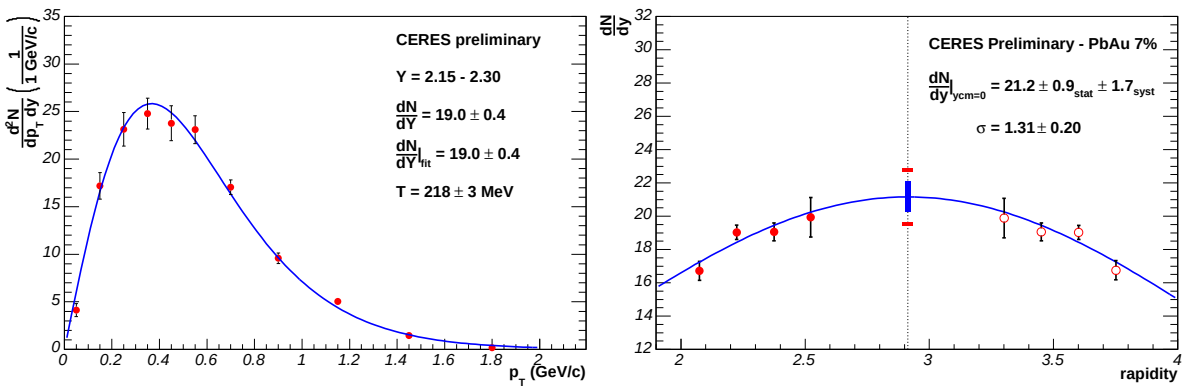

Figure 4. Transverse momentum and rapidity K_S^0 spectra from the K_S^0 analysis performed without PID and without secondary vertex reconstruction [19].

Two independent analyses of the K_S^0 spectra were done using the CERES data [19, 8]. The first one, performed without PID and without secondary vertex reconstruction, is based on TPC information only [19]. A cut in the Armenteros-Podalanski plane was used in order to suppress Λ contamination. The p_T and y spectra are shown in Fig. 4. An alternative approach of the K_S^0 reconstruction was performed without PID but with secondary vertex reconstruction [8] which is already described in Section 3. In both analyses, Pb+Au events taken with the most central trigger were used. The K_S^0 transverse momenta spectrum obtained with this analysis [8] is shown in Fig. 5 (left). The invariant multiplicity was fitted with an exponential fall-off with transverse mass m_t. The yields and the inverse slope parameter T of the p_T spectra from the two analyses are in good agreement. A comparison with results from other experiments is shown in Fig. 5 (right). In order to match the centrality of the CERES experiment, results from the NA49 [20, 21] and NA57 [22] experiments are slightly rescaled. A rather good agreement between the NA49 analysis of charged kaons and the CERES K_S^0 results in shape and yield was found. The difference in the yield is only 5%. The rapidity distribution of K_S^0 observed by NA49 shows a similar shape as the one from CERES (represented with the blue dotted line in Fig. 5 (right)) and a relatively good agreement in the yield. Within the CERES acceptance the results agree with the NA57 data, although the NA57 fit does not.

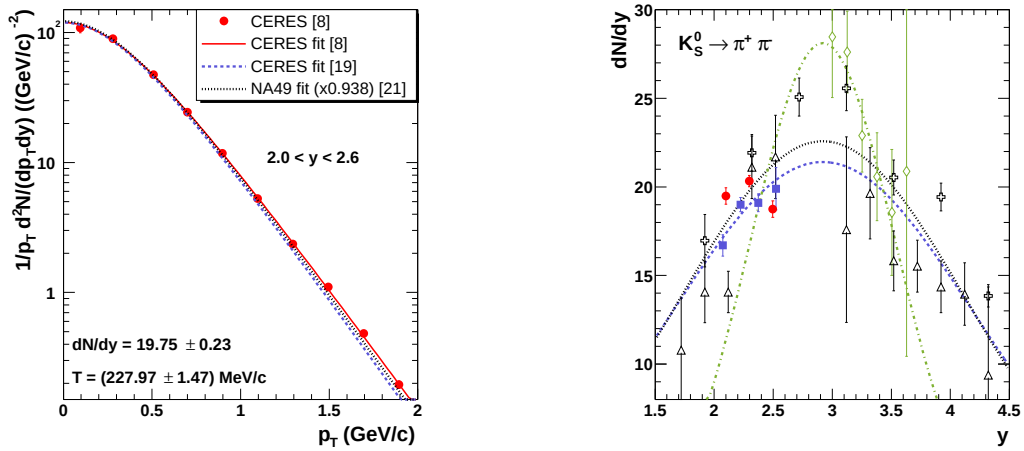

Figure 5. Left: Transverse momentum K^0_S spectrum from the K^0_S analysis performed with secondary vertex reconstruction [8]. Right: A comparison between CERES results (red circles [8] and blue squares [19]), published (open triangles) [20] and preliminary (open crosses) [21] NA49 results and NA57 data (green diamonds) [22]. The black dotted line represents a fit to the charged kaon yield measured by the NA49, while blue (green) dotted line corresponds to a fit to the K^0_S yield measured by the CERES (NA57).

The CERES experiment enabled for the first time at SPS to study simultaneously the leptonic and charged kaon decay modes of the ϕ meson, which may shed light onto the ϕ puzzle [23]. In order to obtain the p_T spectrum of ϕ mesons, the invariant mass distributions of K^+K^- pairs were constructed. The corresponding distributions

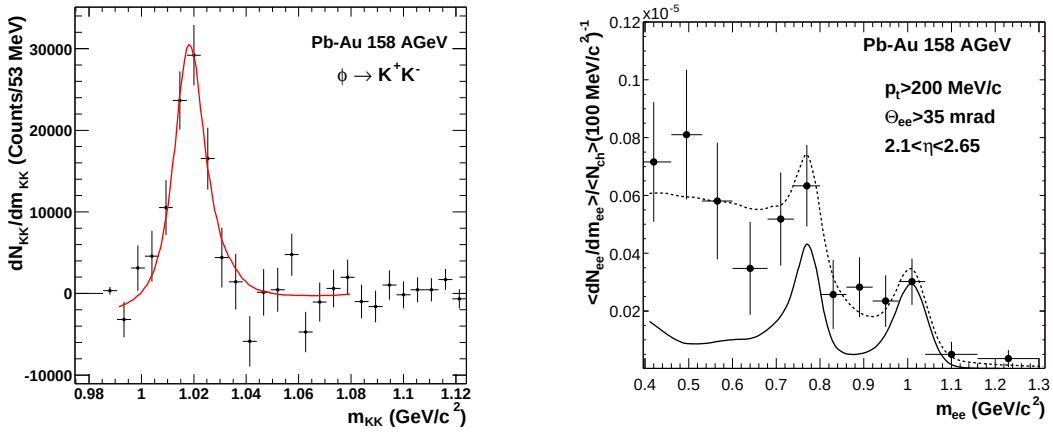

Figure 6. Left: K^+K^- invariant mass spectrum after background subtraction in 1.5 GeV/c $< p_T^{\phi} <$ 1.75 GeV/c and $2.2 < y^{\phi} < 2.4$. Right: e^+e^- invariant mass spectrum compared to the hadron decay cocktail (solid line) and to a model calculation assuming the dilepton yield form the QGP phase and an in medium spread ρ (dashed line).

of the combinatorial background were calculated using the mixed-event technique. An example is shown in Fig. 6 (left). To study ϕ mesons in the dilepton (e^+e^-) decay mode, electrons are identified using the RICH detectors and the TPC dE/dx.

The main difficulties of reconstructing the ϕ meson in the dilepton channel are the low branching ratio and huge combinatorial background. Details of how to reduce the combinatorial background are explained in [5, 24, 25]. The e^+e^- invariant-mass spectrum, corrected for the efficiency and normalized to the number of charged particles in the acceptance is shown in Fig. 6 (right). In the same figure are shown the expectations from the hadron decay cocktail [26], as well as a model calculation where the cocktail ρ contribution is replaced by an explicit in-medium modification combined with continuous $\pi\pi$ annihilation [27]. The later accounts very well for the data. The inverse slope parameter of T =273±9(stat)±10(syst) MeV and a rapidity density dN/dy of 2.05±0.14(stat)±0.25(syst) in the K^+K^- mode and T =306±82(stat)±40(syst) MeV and dN/dy =2.04±0.49(stat)±0.32(syst) in the dilepton mode are in good agreement within errors. The data do not support a possible enhancement of the ϕ yield in the dilepton over the hadronic channel by a factor larger than 1.6 at the 95% CL.

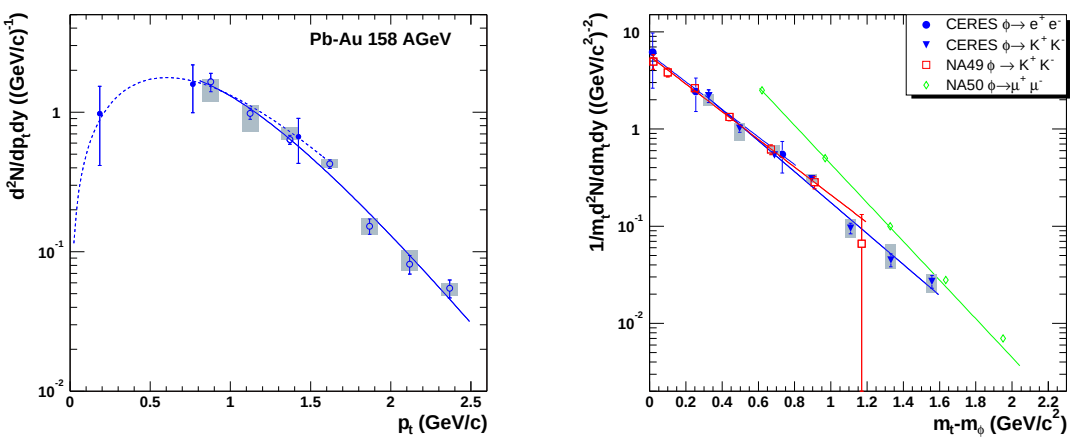

Figure 7. Left: Acceptance and efficiency corrected p_T spectrum of ϕ measured in the K^+K^- (open cycles) and e^+e^- (closed circles) decay modes. Right: Scaled m_T distribution of ϕ mesons reconstructed in the K^+K^- (triangles) and e^+e^- (circles) decay channels compared to the results from NA49 (squares) and NA50 (diamonds).

The p_T dependence of the ϕ meson yield measured in the K^+K^- and e^+e^- decay channels, corrected for the acceptance and efficiency, is shown in Fig. 7 (left). The results are in very good agreement. After accounting for the slightly different measurement conditions, a comparison between CERES results and the existing Pb+Pb systematics [28] is shown in Fig. 7 (right). The CERES results are in good agreement with the results from NA49 measured in the kaon channel. On the other hand, CERES data in the K^+K^- channel do not agree with NA50 results.

References

[1] Ollitrault J-Y 1992 *Phys. Rev.* D **46** 229
[2] Barrette J *et al* [E877 Collaboration] 1994 *Phys. Rev. Lett.* **73** 2532
[3] Poskanzer A M and Voloshin S A 1998 *Phys. Rev.* C **58** 1671
[4] Koch P, Müller B and Rafelski J 1986 *Phys. Rep.* **142** 167

[5] Marín A *et al.* [CERES Collaboration] 2004 *J. Phys.* G **30** S709 (*Preprint* nucl-ex/0406007)
[6] Eidelman S *et al.* [Particle Data Group] 2004 *Phys. Lett.* B **592** 1
[7] Milošević J [CERES Collaboration] 2005 *Proc. Quark Matter, Nucl. Phys.* **A** in print, (*Preprint* nucl-ex/0510057); Milošević J 2006 (Heidelberg University) *Doctoral Thesis* published
[8] Ludolphs W 2006 (Heidelberg University) *Doctoral Thesis*, published
[9] Dinh P M, Borghini N and Ollitrault J-Y 2000 *Phys. Lett.* **B477** 51
[10] Kolb P F, Huovinen P, Heinz U W and Heiselberg H 2001 *Phys. Lett.* **B500** 232
[11] Huovinen P 2005 Private Communication
[12] Kolb P F, Sollfrank J and Heinz U W 1999 *Phys. Lett.* B **459** 667
[13] Stefanek G 2005 [NA49 Collaboration] *Proc. Quark Matter, Nucl. Phys.* **A** in print; (*Preprint* nucl-ex/0510067)
[14] Oldenburg M [STAR Collaboration] 2005 *J. Phys.* G **31** S437
[15] Csőrgő T and Lőrstad B 1996 *Phys. Rev.* C **54** 1390
[16] Csanád M, Csőrgő T and Lőrstad B 2004 *Nucl. Phys.* A **742** 80
[17] Csőrgő T *et al.* 2003 *Phys. Rev.* C **67** 034904
[18] Taranenko A [PHENIX Collaboration] 2005 (*Preprint* nucl-ex/0506019)
[19] Radomski S 2006 (GSI) *Doctoral Thesis* preliminary
[20] Höhne C [NA49 Collaboration] 1999 *Nucl. Phys.* A **661** 485c
[21] Mischke A [NA49 Collaboration] 2002 (*Preprint* nucl-ex/0209002)
[22] Antinori F *et al.* [NA57 Collaboration] 2005 *J. Phys.* G **31** 1345
[23] Marín A *et al.* [CERES Collaboration] 2006 *Phys. Rev. Lett.* **96** 152301 (*Preprint* nucl-ex/0512007)
[24] Mískowiec D [CERES Collaboration] 2005 *Proc. Quark Matter Nucl. Phys.* **A** in print, (*Preprint* nucl-ex/0511010)
[25] Yurevich S 2006 (Heidelberg University) *Doctoral Thesis*, published
[26] Sako H [CERES Collaboration] 2000 *Technical Report* **03-25**
[27] Rapp R and Wambach J 2000 *Adv. Nucl. Phys.* **25** 1; Rapp R 2005 Private Communication; Braaten E, Pisarski R D and Yuan T-C 1990 *Phys. Rev. Let.* **64** 2242
[28] Röhrich D 2001 *J. Phys.* G **27** 355